https://doi.org/10.5194/bg-2020-289
Preprint. Discussion started: 26 August 2020

Biogeosciences Discussions
Open Access
EGU

A bottom-up quantification of foliar mercury uptake fluxes across Europe

Lena Wohlgemuth[1,*], Stefan Osterwalder[2], Carl Joseph[1], Ansgar Kahmen[1], Günter Hoch[1], Christine Alewell[1], Martin Jiskra[1,*]

[1]Department of Environmental Sciences, University of Basel, Basel, Switzerland
[2]Institut des Géosciences de l'Environnement, Université Grenoble Alpes, CNRS, IRD, Grenoble INP, Grenoble, France

[*]Correspondence to: lena.wohlgemuth@unibas.ch; martin.jiskra@unibas.ch

Abstract. The exchange of gaseous elemental mercury, Hg(0), between the atmosphere and terrestrial surfaces remains poorly understood mainly due to difficulties in measuring net Hg(0) fluxes on the ecosystem scale. Emerging evidence suggests foliar uptake of atmospheric Hg(0) to be a major deposition pathway to terrestrial surfaces. Here, we present a bottom-up approach to calculate Hg(0) uptake fluxes to aboveground foliage by combining foliar Hg uptake rates normalized to leaf area with species-specific leaf area indices. This bottom-up approach incorporates systematic variations in crown height and needle age. We analyzed Hg content in 583 foliage samples from six tree species at 10 European forested research sites along a latitudinal gradient from Switzerland to Northern Finland over the course of the 2018 growing season. Foliar Hg concentrations increased over time in all six tree species at all sites. We found that foliar Hg uptake rates normalized to leaf area were highest at the top of the tree crown. Foliar Hg uptake rates decreased with needle age of multi-year old conifers (spruce and pine). Average species-specific foliar Hg uptake fluxes during the 2018 growing season were 18 ± 3 µg Hg m^{-2} for beech, 26 ± 5 µg Hg m^{-2} for oak, 4 ± 1 µg Hg m^{-2} for pine and 11 ± 1 µg Hg m^{-2} for spruce. For comparison, the average Hg(II) wet deposition flux measured at 5 of the 10 research sites during the same period was 2.3 ± 0.3 µg Hg m^{-2}, which was four times lower than the site-averaged foliar uptake flux of 10 ± 3 µg Hg m^{-2}. Scaling up site-specific foliar uptake rates to the forested area of Europe resulted in a total foliar Hg uptake flux of approximately 20 ± 3 Mg during the 2018 growing season. Considering that the same flux applies to the global land area of temperate forests, we estimate a foliar Hg uptake flux of 108 ± 18 Mg. Our data indicate that foliar Hg uptake is a major deposition pathway to terrestrial surfaces in Europe. The bottom up approach provides a promising method to quantify foliar Hg uptake fluxes on an ecosystem scale.

https://doi.org/10.5194/bg-2020-289
Preprint. Discussion started: 26 August 2020

1 Introduction

Mercury (Hg) is a toxic pollutant ubiquitous in the environment due to long-range atmospheric transport. Anthropogenic emissions of Hg into the atmosphere mainly originate from burning of coal, artisanal and small-scale gold mining and non-ferrous metal and cement production while geogenic emission occur from volcanoes and rock weathering (UN Environment, 2019). Atmospheric Hg is deposited to terrestrial surfaces and the ocean and can be re-emitted back to the atmosphere (Bishop et al., 2020; Obrist et al., 2018). The residence time of Hg in the atmosphere and its transfer to land and ocean surfaces mainly depends on its speciation (Driscoll et al., 2013). Gaseous elemental mercury Hg(0) is the dominant form (> 90 %) of atmospheric Hg (Sprovieri et al., 2017), exhibiting a residence time of several months to more than a year (Ariya et al., 2015; Saiz-Lopez et al., 2018). Atmospheric Hg will ultimately be transferred to water and land surfaces by wet or dry deposition. In the wet deposition process, Hg(0) is oxidized in the atmosphere to water-soluble Hg(II) and washed down to the Earth surface by precipitation (Driscoll et al., 2013). Wet deposition fluxes of Hg(II) to terrestrial surfaces are well constrained and direct measurements are coordinated in regional and international atmospheric deposition monitoring programs (EMEP, NADP) (EMEP, 2016; Prestbo and Gay, 2009; Wängberg et al., 2007; Weiss-Penzias et al., 2016).

Dry deposition fluxes of Hg(0) and Hg(II) to the earth surface are less constrained owing to challenges in measuring net ecosystem exchange fluxes (Driscoll et al., 2013; Zhang et al., 2009) and atmospheric Hg(II) concentrations (Jaffe et al., 2014). The dry deposition of Hg can occur by vegetation uptake and subsequent transfer to the ground via litterfall (Risch et al., 2017; Wang et al., 2016), by wash-off from foliar surfaces via throughfall (Wright et al., 2016) or by direct deposition to terrestrial surfaces and soils (Obrist et al., 2014). Hg dry deposition is not routinely monitored by most environmental programs. Consequently, atmospheric mercury models inferring Hg dry deposition across Europe during summer months lack observational constraints (Gencarelli et al., 2015). Ecosystem scale mass balance studies, however, revealed that litterfall deposition to forest floors exceeds wet deposition (Bushey et al., 2008; Demers et al., 2007; Graydon et al., 2006; Grigal, 2002; Rea et al., 2002; Risch et al., 2012, 2017; St. Louis et al., 2001; Teixeira et al., 2012; Zhang et al., 2016). Several lines of evidence suggest that uptake of atmospheric Hg(0) by vegetation represents an important process in terrestrial Hg cycling: i) isotopic fingerprinting studies revealed that approximately 90 % of Hg in foliage and 60 % – 90 % of Hg in soils originate from atmospheric Hg(0) uptake by vegetation (Demers et al., 2013; Enrico et al., 2016; Jiskra et al., 2015; Zheng et al., 2016), ii) observations of foliar Hg concentrations increase with exposure time to atmospheric Hg(0) (Assad et al., 2016; Ericksen and Gustin, 2004; Fleck et al., 1999; Frescholtz et al., 2003; Laacouri et al., 2013; Millhollen et al., 2006; Rea et al., 2002) while Hg uptake via the root system was found to be minor (Assad et al., 2016; Frescholtz et al., 2003; Millhollen et al., 2006), iii) atmospheric Hg(0) correlates with the photosynthetic activity of vegetation suggesting that summertime minima in atmospheric Hg(0) in the Northern hemisphere are controlled by vegetation uptake (Jiskra et al., 2018; Obrist, 2007)

The exact mechanism of the atmosphere-foliar Hg(0) exchange is not yet fully understood. Laacouri et al. (2013) observed highest Hg concentrations in leaf tissues as opposed to leaf surfaces and cuticles, implying that Hg(0) diffuses into the leaves. Exposing plants to Hg(0) in form of enriched Hg isotope tracers, Rutter et al. (2011) found that plant Hg uptake was mainly to the leaf interior. Leaf Hg content correlated with stomatal density (Laacouri et al., 2013) suggesting that stomatal uptake represents the main pathway. Nonstomatal uptake was observed by Stamenkovic and Gustin (2009) under conditions of reduced stomatal aperture implying adsorption of atmospheric Hg to cuticles surfaces. Re-emission of Hg from foliage can occur by photoreduction of Hg(II) to Hg(0) and

https://doi.org/10.5194/bg-2020-289
Preprint. Discussion started: 26 August 2020

subsequent volatilization (Graydon et al., 2006). The re-emission potential of Hg previously taken up by foliage and strongly complexed in plant tissue (Manceau et al., 2018) was suggested to be lower than the re-emission potential of surface-bound Hg (Jiskra et al., 2018; Yuan et al., 2019).

Hg contents in foliage were shown to be species-specific (Blackwell and Driscoll, 2015; Laacouri et al., 2013; Navrátil et al., 2016; Obrist et al., 2012; Rasmussen et al., 1991). It is currently unresolved if deciduous broad leaves accumulate higher Hg concentrations than needles (Blackwell and Driscoll, 2015; Navrátil et al., 2016) or if it is the other way around (Hall and St. Louis, 2004; Obrist et al., 2011, 2012). Deciduous species shed their leaves at the end of the growing season, whereas most conifers grow needles over multiple years and continue to accumulate Hg, resulting in increasing Hg concentrations with needle age (Hutnik et al., 2014; Navrátil et al., 2019; Ollerova et al., 2010). Furthermore, Hg concentrations in foliage have been shown to vary within the canopy (Bushey et al., 2008). Physiological differences between deciduous and coniferous tree species and inconsistent sampling of needle age and canopy height may have contributed to the uncertainty in literature whether deciduous or coniferous species take up more Hg.

The goal of this study was to improve the understanding of foliar Hg(0) uptake and quantify foliar uptake fluxes at European forest research sites. The objectives were to: 1) determine the temporal evolution of Hg concentrations and the Hg pool in foliage of 6 tree species at 10 European research sites along a south-north transect from Switzerland to Finland over the 2018 growing season, 2) investigate the effect of needle age, crown height and tree functional group on foliar Hg uptake, 3) quantify foliar Hg uptake fluxes per m^2 ground surface area based on the temporal evolution of the foliar Hg pool over the growing season. 4) estimate the foliar uptake fluxes for Europe and temperate forests globally by scaling up species-averaged foliar uptake rates determined in this study to respective forest areas.

2 Materials and Methods

2.1 Site description

Foliage samples were collected from 10 European research sites located along a south-north transect from Switzerland to Scandinavia (Fig. 1). The Hölstein site in Switzerland comprises the Swiss Canopy Crane II (SCCII) operated by the Physiological Plant Ecology Group of the University of Basel (Kahmen et al., 2019). Our principal site Hölstein allowed to systematically access the entire canopy through the gondola of a crane. The research sites Schauinsland and Schmücke are part of the air monitoring network of the German Federal Environment Agency (UBA) (Schleyer et al., 2013). Hyltemossa, Norunda, Svartberget and Pallas are Integrated Carbon Observation System (ICOS) sites operated by Lund University (LU), the Swedish University of Agricultural Sciences (SLU) and the Finnish Meteorological Institute (FMI) (Lindroth et al., 2015, 2018; Lohila et al., 2015). Hurdal is a prospective ICOS Ecosystem station, an ICP Forests Level II Plot and a European Monitoring and Evaluation Programme (EMEP) air measurement site operated by the Norwegian Institute of Bioeconomy Research (NIBIO) and the Norwegian Institute for Air Research (NILU) (Lange, 2017). Bredkälen and Råö are Swedish EMEP air measurement sites operated by the Swedish Environmental Research Institute (IVL) (Wängberg et al., 2016; Wängberg and Munthe, 2001). Tree species composition differed between sites. Hölstein, for instance, is a mixed forest harbouring 14 different tree species while Hyltemossa is an exclusive

https://doi.org/10.5194/bg-2020-289
Preprint. Discussion started: 26 August 2020

spruce stand (see Table S5 for details). At 5 locations (Schauinsland, Schmücke, Råö, Bredkälen and Pallas) Hg(II) wet deposition measurements were performed by the operators of the research sites.

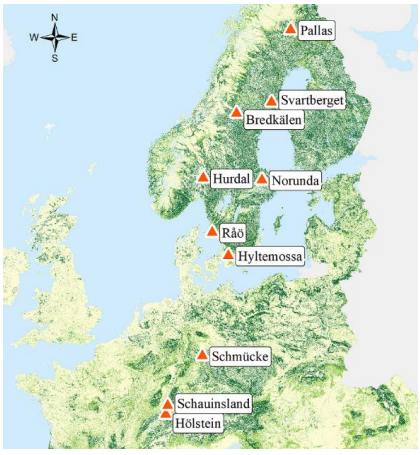

Fig. 1: Research sites for foliage sampling during the 2018 growing season. Base map corresponds to the Joint Research Centre (JRC) Pan-European Forest Type Map 2006 (JRC, 2010; Kempeneers et al., 2011). Reuse is authorized under reuse policy of the European Commission (EU, 2011).

2.2 Sample collection

Foliage sampling strategy was guided by the ICP Forests Programme sampling manual (Rautio et al., 2016), requesting to take samples that have developed under open sunlight from the top third of the crown canopy. At 4 sites (Svartberget, Hyltemossa, Norunda and Hölstein) we complied with the ICP Forest sampling protocol. At 6 sites (Pallas, Bredkälen, Hurdal, Råö, Schmücke and Schauinsland) we had to adapt the sampling strategy to local conditions and available equipment. At our focus research site in Hölstein, Switzerland a crane allowed access to the top of the crown and vertical sampling of beech, oak and spruce. Since pine did not grow needles at ground level we did not sample their vertical profiles. Vertical sampling of spruce needles in Hölstein during 2018 was repeated in 2019 with five spruce trees because only two spruce trees had been sampled during 2018 of which one died from drought induced stress by the end of the 2018 growing season (Schuldt et al., 2020). The relative effect of height on Hg accumulation in Hölstein spruce needles is therefore investigated with data from the growing season 2019. Samples at Hyltemossa and Svartberget were cut from tree canopies using a 20 m telescopic scissors and at Hurdal using a 3 m telescopic scissors. At Norunda samples were shot from the tree canopies using a shotgun. At Schauinsland, Schmücke, Råö and Bredkälen we used a 5 m telescopic scissors for cutting the branches in the lower half of the crown. At Pallas and Råö branches were cut from low-growing trees at breast height. We collected intact leaves at three to six time points during the 2018 growing season. Samples from at least three different branches of the same tree were pooled to a composite sample. We sampled at least three trees per species (one to four species) with the exception of Råö where only one oak and one spruce tree were available. Sampling and sample preparation was conducted using clean nitryl gloves. Leaves were cut from outermost branches. All samples were stored in Ziplock bags in the freezer until analysis. Sampling dates are reported in Table S1 for each site. At Hölstein atmospheric Hg(0) was measured integrated over the whole sampling period by using passive air samplers (PAS) as described by McLagan et al. (2016). PAS were exposed at ground level

https://doi.org/10.5194/bg-2020-289
Preprint. Discussion started: 26 August 2020

(1.6 m) under the canopy at four locations on the plot and additionally at three heights of 10 m, 19 m and 35 m on the crane railing (details in S7 and Fig. S4) from 15 May 2018 to 18 October 2018. The PAS air measurement campaign at Hölstein was repeated in 2019 with PAS exposed at 1.5 m, 10 m, 19 m and 35 m height at the crane from 16 May 2019 to 12 September 2019. Measurement of one of the PAS installed at 10 m height in 2019 was excluded from further analysis because it produced an implausible high result which can probably be traced back to a measurement error. Under dry conditions at noon time on 17 July 2019 we measured stomatal conductance to water vapor of beech, pine and oak from the crane gondola at Hölstein using an SC-1 Leaf Porometer (Meter Group, Inc. USA).

2.3 Sample preparation and measurements

In total 584 leaf samples were collected, weighted and analyzed for leaf mass per area (LMA) and subsequently dried and grinded for Hg concentration analysis. The projected leaf area was measured using a LI3100 Area Meter (LI-COR Biosciences USA). We performed duplicate scans of 17 % of foliage samples and obtained a mean per cent deviation between scans and respective duplicate scans of 3 % ± 3 %. For measuring projected needle area, we calibrated the LI3100 with rubberized wires of known length and a diameter of 1.74 ± 0.02 mm (see S4 and Fig. S2). For the two sites Hurdal and Pallas the performance and resolution of the LI3100 was insufficient and unrealistic results were discarded and median values from literature were used instead (see S4 for details). For the three ICOS sites Hyltemossa, Norunda and Svartberget we obtained LMA values measured by research staff according to ICOS protocol (Loustau et al., 2018) (Sect. S4). Foliage samples were oven-dried at 60°C for 24 h. We did not observe any Hg losses irrespective of drying temperatures of 25°C, 60°C and 105°C (Fig. S1). A similar result was obtained by Yang et al. (2017) for Hg in wood and by Lodenius et al. (2003) for Hg in moss. Dried samples were weighted and homogenously grinded in an ordinary stainless steel coffee grinder. Total Hg concentrations were measured with atomic absorption spectrophotometry using a direct mercury analyzer (DMA-80 Hg, Heerbrugg, Switzerland). Standard Reference Materials (SRMs) used in this study were NIST-1515 apple leaves and spruce needle sample B from the 19th ICP Forests needle/leaf interlaboratory comparison. Standard measurement procedures included running a quality-control pre-sequence consisting of three method blanks, one process blank (wheat flour) and three liquid primary reference standards (PRS; 50 mg of 100 ng/g NIST-3133 in 1 % BrCl). Daily performance of the instrument was assessed based on the three liquid PRS and all data were corrected accordingly if the measured PRS were within 90 % to 110 % of the expected value. If PRS were outside this acceptable range, the instrument was re-calibrated. Each sequence consisted of four SRMs, one process blank consisting of commercial wheat flour and 35 samples. Sequences were rejected if one SRM value was outside of the certified uncertainty range (NIST-1515) or 10 % of the respective target concentration (ICP Forests spruce B) or if the absolute Hg content of the flour blank was > 0.3 ng. The average recovery for Hg during measurement of all samples in this study was 99.9 % ± 4.0 % (mean ± sd) (n = 15) for NIST-1515 and 101.6 % ± 6.9 % (mean ± sd) (n = 40) for ICP Forests spruce B. The process blanks exhibited an average Hg content of 0.10 ng ± 0.09 ng (mean ± sd) (n = 23). As an additional quality control, we passed the 21st and 22nd ICP Forests needle/leaf interlaboratory comparison test 2018/2019 and 2019/2020 for Hg.

2.4 Bottom-up calculation of foliar Hg uptake fluxes

Foliar Hg concentration (µg Hg $g^{-1}_{d.w.}$) of each leaf/needle sample was multiplied with the respective sample leaf mass per area (LMA; $g_{d.w.}$ m^{-2} $_{leaf}$) to obtain foliar Hg content normalized to leaf area (µg Hg m^{-2} $_{leaf}$). Foliar Hg uptake rates ($uptakeR_{leaf\ area}$; µg Hg m^{-2} $_{leaf}$ $month^{-1}$) for each tree species were derived from the change in Hg

https://doi.org/10.5194/bg-2020-289
Preprint. Discussion started: 26 August 2020

content normalized to leaf area over time (3 to 6 points in time) using a linear regression fit. Linear regression was performed applying an ordinary least square model in the Python module statsmodels (Python 3.7.0). Linear regression parameter (R^2) of each site and tree species are summarized in Table S1. Foliar Hg uptake fluxes ($uptakeF_{ground\ area}$; µg Hg m^{-2}_{ground} $month^{-1}$) per ground surface area were calculated by multiplying the foliar Hg uptake rates ($uptakeR_{leaf\ area}$) with species-specific leaf area indices (LAIs; $m^2_{\ leaf\ area}$ $m^{-2}_{\ ground}$) in order to obtain foliar Hg uptake fluxes normalized to ground surface area:

$$uptakeF_{ground\ area} = uptakeR_{leaf\ area} * LAI \quad (1)$$

Fig. ***2*** illustrates this flux calculation schematically. We used species-specific LAIs retrieved from a global data base provided by Iio and Ito (2014). In total, 205 values of one-sided LAIs measured in Central Europe and Scandinavia between a latitude of 46° N and 63° N and published in peer-reviewed journals were selected for calculating an average LAI value of each species. Species-specific average LAI values are displayed in Table S2. All LAI values for each species are peak-season values. To calculate the foliar uptake flux over the growing season, the average daily uptake flux was multiplied by the length of the growing season in days. For each site, the growing season length in days, which depends on the latitude of the site, was obtained from Garonna et al. (2014); Rötzer and Chmielewski (2001) (Table S1). The approximate relative abundance of sampled tree species (Table S5) at the four research sites Hölstein, Hyltemossa, Norunda and Svartberget were obtained by research staff (pers. communication). We calculated the total foliar Hg uptake flux for these four research sites as the sum of species-specific foliar Hg uptake fluxes of all locally dominant tree species multiplied by their relative abundance (Table S5).

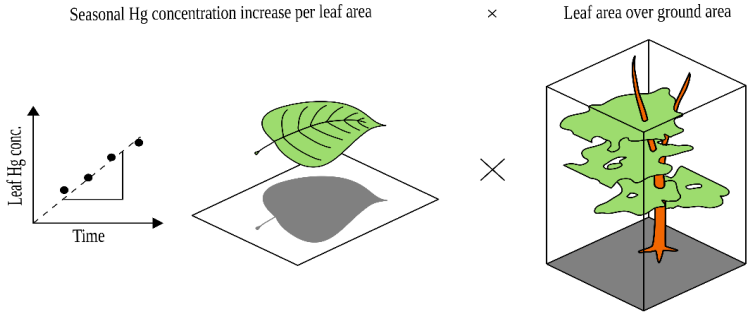

Fig. 2: Bottom-up approach (Eq. 1) for calculating foliar Hg uptake flux per ground area (uptakeF; ng Hg m^{-2}_{ground} $month^{-1}$). The linear regression slope of leaf Hg concentration (ng Hg $g_{d.w.}$) over time is multiplied with the respective sample leaf mass per area (LMAs; $g_{d.w.}$ $m^{-2}_{\ leaf\ area}$). The resulting foliar Hg uptake rate per leaf area ($uptakeR_{leaf\ area}$; ng Hg m^{-2}_{leaf} $month^{-1}$) is then multiplied with the species-specific leaf area index (LAI; $m^2_{\ leaf\ area}$ $m^{-2}_{\ ground}$).

2.5 Correction factor for needle Hg uptake flux as function of needle age

At all sites, we investigated Hg concentrations in multi-year pine and spruce needles from the current season (y_0, needles sprouting in spring of the sampling year) and in one-year old needles (y_1, needles sprouting in the year prior to the sampling year). At 5 sites (Bredkälen, Hölstein, Hyltemossa, Schauinsland and Schmücke) we additionally sampled two-year old (y_2) and three-year old (y_3) spruce needles. Sampling and measuring Hg uptake in all needle age classes of a conifer tree is time-consuming and costly. In standard forest monitoring programs young needles from age class y_0 or y_1 are usually sampled. We determined a species-specific age correction factor (cf_{age}) to relate the needle uptake of an entire coniferous tree to the current season (y_0) needles. The factor cf_{age}

https://doi.org/10.5194/bg-2020-289
Preprint. Discussion started: 26 August 2020

was derived from Hg measurements of 316 needle samples of different age classes using i) the evaluated relative Hg accumulation rate (RAR; Eq. 2), which represents the Hg accumulation of each needle age class normalized to the Hg accumulation rate in current season (y_0), and ii) the respective relative biomass (RB) of each needle age class to the total needle biomass from literature determined by Matyssek et al. (1995). Needles used to determine the RAR were sampled by the Bavarian State Institute of Forestry at 11 ICP Forests plots in Bavaria, Germany in 2015 and 2017. Needle samples from 2015 consisted of 33 batches of spruce and 6 batches of pine samples. Needle samples from 2017 consisted of 32 batches of spruce and 6 batches of pine samples. For spruce needles, each batch was composed of samples of age class y_0 to age class y_3, of which 7 spruce needle batches were composed of samples of age class y_0 to y_5 and 6 spruce needle batches of age class y_0 to y_6. For pine needles, each batch of the two sampling years 2015 and 2017 was composed of samples of age class y_0 to y_1 and one pine needle batch was additionally composed of samples of age class y_2. The RAR of spruce and pine samples of different needle years (y_i, i = 1, 2, …, n) in each sample batch of the sampling years 2015 and 2017 was calculated as follows:

$$RAR_{y_i} = \frac{c_{Hg}(y_i) - c_{Hg}(y_{i-1})}{c_{Hg}(y_0)} \quad (2)$$

Resulting average RARs of the spruce and pine needle samples together with the RB are presented in Table S3. For each needle age class the factor cf_{age} calculates as

$$cf_{age} = 1 * RB_{y_0} + RAR_{y_1} * RB_{y_1} + \ldots + RAR_{y_n} * RB_{y_n} \quad (3)$$

In accordance to our bottom-up approach for calculating the foliar Hg uptake flux (Eq. 1) the modified flux calculation for conifers is:

$$uptakeF_{ground\ area} = cf_{age} * uptakeR_{y0;\ needle\ area} * LAI \quad (4)$$

Final values of cf_{age} are summarized in Sect. S6, Table S3.

2.6 Correction factor for foliar Hg uptake flux as function of crown height

Standard foliage sampling in forest monitoring programs is from the top third of the crown (Rautio et al., 2016). We determined a species-specific height correction factor (cf_{height}) allowing to scale up the treetop foliar Hg uptake flux to whole-tree foliage. The species-specific height correction factor equals the multiplication of two ratios: i) the ratio $r_{conc.coeff.}$ of the linear regression coefficient (ng Hg $g^{-1}_{d.w.}$ $month^{-1}$) of Hg concentrations in foliar samples over the growing season at ground/mid canopy level to the equivalent coefficient at top canopy level and ii) the ratio r_{LMA} of average LMA at ground/mid canopy level to the average LMA at top canopy level (Eq 5).

$$cf_{height} = r_{conc.\ coeff.} * r_{LMA} = \frac{conc.\ coeff._{\cdot ground}}{conc.\ coeff._{\cdot top\ canopy}} * \frac{LMA_{ground}}{LMA_{top\ canopy}} \quad (5)$$

According to ecosystem models on light attenuation and photosynthesis in tree canopies (Hirose, 2004; Körner, 2013; Monsi and Saeki, 2004) the 3 top canopy layers of leaf area intercept almost 90 % of available sunlight leaving the lower leaf layers with reduced light. We thus assume that the top 3 canopy layers of leaf area index (LAI; $m^2_{leaf\ area}$ m^{-2}_{ground}) mainly consist of sun-adapted foliage (i.e. sun-leaves) with Hg uptake rates corresponding to the uptake rates measured at top canopy. Leaf area indices and vertical foliar biomass distribution differ between tree species (Fichtner et al., 2013; Hakkila, 1991; Sharma et al., 2016; Tahvanainen and Forss, 2008; Temesgen et al., 2005). We did not apply a height correction for tree species with a LAI $\leq$ 3. For tree species with leaf area

https://doi.org/10.5194/bg-2020-289
Preprint. Discussion started: 26 August 2020

indices > 3 we assumed the following species-specific foliar Hg uptake flux of the whole tree foliage (uptakeF) in extension of Eq. (1):

$$uptakeF_{ground\ area}\ [ng\ Hg\ m^{-2}_{ground}\ month^{-1}] = uptakeR_{top\ canopy;\ \ leaf\ area} * \left(3 + \ cf_{height} * (LAI - 3)\right) \quad (6)$$

Final values of cf_{height} are summarized in Sect. S9, Table S4.

3 Results and Discussion

3.1 Effect of needle age on foliar Hg uptake

Spruce and pine revealed increasing Hg concentration with needle age at all sites (Fig. S5). In order to demonstrate the increase in Hg concentration with needle age class, we display results from Hölstein, Hyltemossa and Schauinsland (Fig. 3). The average late season Hg concentration in one-year old (y_1) spruce needles was by a factor of 1.8 ± 0.4 (mean ± sd between all sites) times higher than the average late season Hg concentration in current season (y_0) spruce needles. From spruce needle age class y_2 to y_1 the ratio of average Hg concentrations was 1.3 ± 0.1 and from y_3 to y_2 1.4 ± 0.1. For pine the corresponding ratio was 1.9 ± 0.2 (mean ± sd between all sites) from y_1 to y_0 needles. Consequently, needle Hg concentrations in spruce and pine almost doubled from the season of sprouting to the subsequent growing season one year later. Needles older than one year (y_2, y_3) continue to accumulate Hg albeit at a slower rate than younger needles (y_0, y_1). This finding is in agreement with previous studies that reported positive trends of Hg concentration in spruce needles from age class y_1 to y_4 (Hutnik et al., 2014; Navrátil et al., 2019; Ollerova et al., 2010).

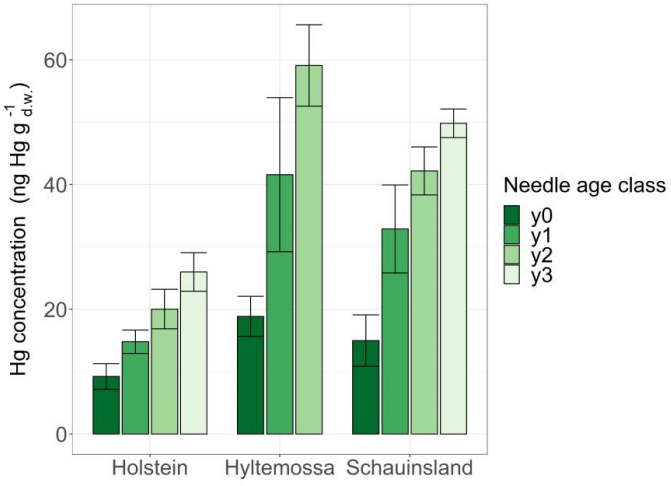

Fig. 3: Hg concentrations (ng g^{-1} d.w.) in spruce needles of four different age classes sampled at 3 research sites (Hölstein, Hyltemossa and Schauinsland) at the end of the 2018 growing season (October – November). Age class y_0 represents current season needles, age classes y_1, y_2 and y_3 one-, two- and three-year old needles, respectively. Error bars denote one standard deviation of samples taken from multiple trees at each site.

We systematically investigated age dependency of Hg accumulation rates using 292 spruce and 24 pine needle samples of age class y_0 to y_6 sampled by the Bavarian State Institute of Forestry in 2015 and 2017 (Sect. 2.5). The relative accumulation rate (RAR) represents the Hg accumulation of an individual needle age class normalized to the respective Hg accumulation rate in the current season y_0 needles (Eq. 2). Needles of all age classes continue

https://doi.org/10.5194/bg-2020-289
Preprint. Discussion started: 26 August 2020

to accumulate Hg, which is in concurrence with our 2018 Hg concentrations of needles y_0 to y_3 (Fig. 3). However, RAR decrease with needle age (Fig. 4). Assuming a linear decline in Hg uptake with spruce needle age, the mature needles (y_n) took up -0.17 ± 0.03 (linear regression coefficient ± se) in 2015 and -0.10 ± 0.02 (linear regression coefficient ± se) in 2017 than the previous age class y_{n-1}. The negative linear trend of pine needle Hg uptake was -0.18 ± 0.02 (linear regression coefficient ± se) in 2015 samples (from y_0 to y_2 Hg uptake) and -0.17 (linear regression coefficient) in 2017 samples (from y_0 to y_1 Hg uptake).

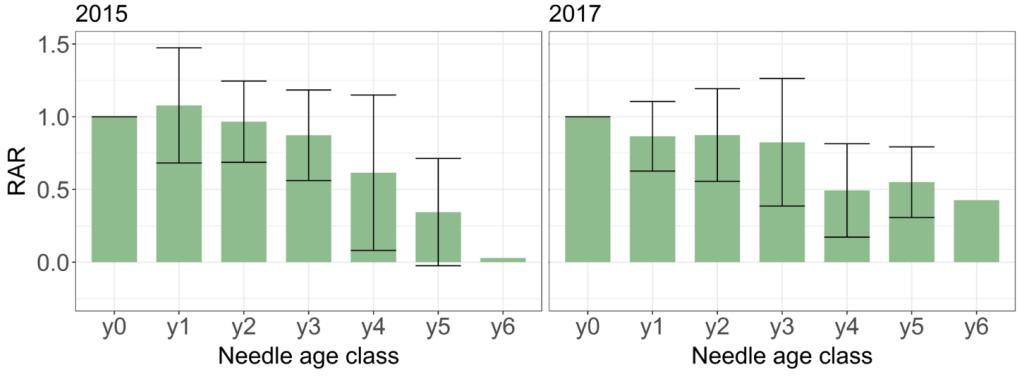

Fig. 4: Average relative Hg accumulation rates (RAR) of 292 spruce needle samples of age class y_0 and y_6 taken by the Bavarian State Institute of Forestry in the two sampling years 2015 (left) and 2017 (right). The RAR represents the ratio of average Hg accumulation rate of the respective needle age class to the Hg accumulation of needle age class 0 (y_0). Error bars denote one standard deviation between RAR of needles sampled from multiple trees and sites.

The decline of Hg RAR with age could be related to a decrease in physiological activity with needle age. The rate of photosynthesis and stomatal conductance decreases in older needles (Freeland, 1952; Jensen et al., 2015; Op de Beeck et al., 2010; Robakowski and Bielinis, 2017; Warren, 2006; Wieser and Tausz, 2007). Consequently, a physiologically less active older needle accumulates less Hg(0). Additionally, adsorption of Hg(0) to needle wax layers as a possible nonstomatal uptake pathway might be minimized in older needles because ageing needles suffer from cuticular wax degradation (Burkhardt and Pariyar, 2014; Güney et al., 2016). As older needles exhibited higher Hg concentrations than younger needles, the Hg re-emission flux might increase with age. Differences of Hg RARs between sampling years 2015 and 2017 (Fig. 4) could be the result of climatic conditions during the two years like precipitation rates, temperature or vapor pressure deficit which impacts needle stomatal conductance and possibly stomatal Hg(0) uptake (Blackwell et al., 2014).

From RAR values of our systematic needle analysis (Fig. 4) we calculated needle age correction factors (cf_{age}) according to Eq. (3) in order to scale up Hg uptake fluxes determined for y_0 needles to Hg uptake fluxes in needles of all age classes (Eq. 4). The correction factor cf_{age} was 0.79 ± 0.03 (factor according to Eq. 3 ± se) for spruce and 0.87 ± 0.06 (factor according to Eq. 3 ± se) for pine (see S6 for details).

3.2 Effect of crown height on foliar Hg content

Foliar Hg concentration, leaf mass per area (LMA) and Hg content normalized to leaf area measured at Hölstein exhibited vertical variation with crown height (Fig. 5). In the following, we discuss all data relative to values measured at top canopy. Top canopy represents the foliage sampling height at the sun-exposed treetop, mid canopy describes the middle height range of sampled trees and ground level represents chest height (1.5 m).

https://doi.org/10.5194/bg-2020-289
Preprint. Discussion started: 26 August 2020

Biogeosciences
Discussions
Open Access
EGU

303 Hg concentrations of beech (Fig. 5a), oak and spruce were lower in top canopy foliage than in foliage growing at
304 ground level. By the end of the growing season (October), average Hg concentration in top canopy (33 – 38 m)
305 beech leaves was 0.84 times and 0.72 times the average Hg concentration at mid canopy (18 – 21 m) and ground
306 level (1.5 m) respectively. For oak, the ratio of average Hg concentrations in top canopy (28 – 38 m) leaves to
307 mid canopy (19 – 22 m) leaves was 0.92 and for current season spruce needles the respective ratio was 0.85 from
308 top canopy (43 - 47 m) to mid canopy (25 - 34 m) needles (spruce needles sampled in September 2019, see 2.2).

309 LMA of foliage samples from top canopies was higher than LMA of foliage samples from lower tree heights (Fig.
310 5b exemplary for beech). The season-averaged LMA ratio of top canopy foliar samples to ground foliar samples
311 was 2.9 for beech, 1.3 for oak and 1.6 for spruce.

312 Because of the large vertical LMA gradient, foliar Hg content normalized to leaf area exhibited an opposite
313 vertical gradient with tree height compared to Hg concentrations (Fig. 5c exemplary for beech). By the end of the
314 growing season Hg content normalized to leaf area in top canopy (33 – 38 m) beech leaves was 1.17 times the Hg
315 content per area in mid canopy (18 – 21 m) and 1.91 times in ground level (1.5 m) leaves. The equivalent ratio of
316 Hg content per area in oak leaves was 1.13 from top canopy (28 – 38 m) to mid canopy (19 – 22 m) and 1.55 for
317 spruce needles from top (43 - 47 m) to mid canopy (25 - 34 m).

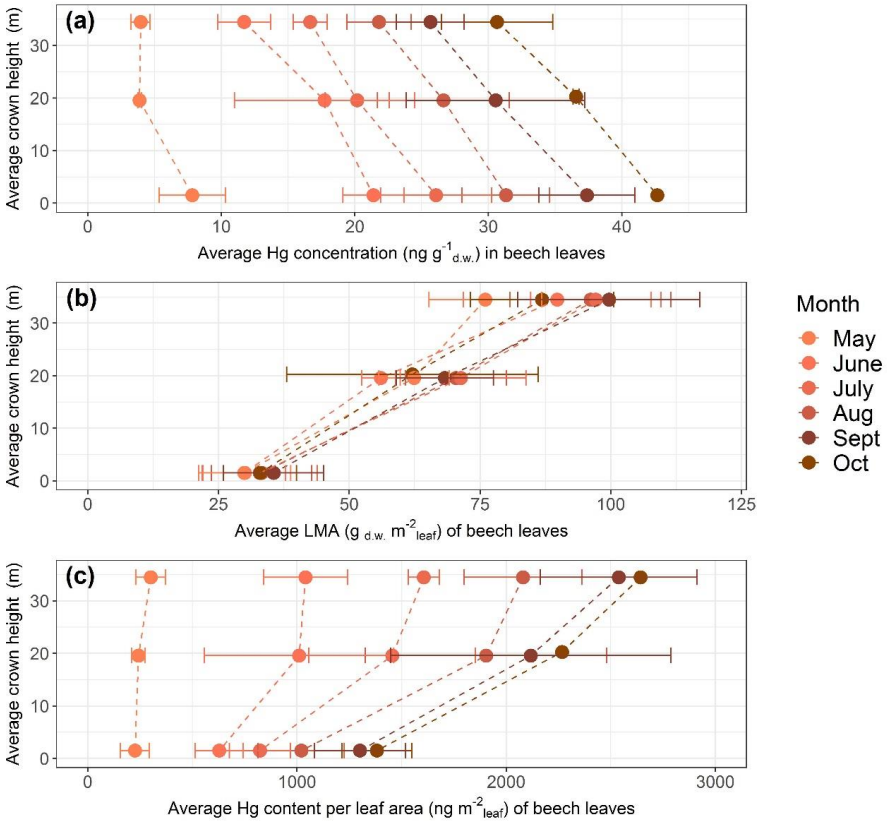

318

319 **Fig. 5: Average values of beech leaf parameters as a function of average tree crown height in meters above ground level**
320 **at Hölstein, Switzerland over the course of the 2018 growing season: a) Hg concentrations (ng Hg $g^{-1}_{d.w.}$), b) leaf mass**
321 **per area (LMA; g^{1} m^{-2}_{leaf} d.w.), c) Hg content normalized to projected leaf area (ng Hg m^{-2}_{leaf}). Error bars denote one**
322 **standard deviation of leaf samples from multiple beech trees (n = 3 – 5).**

https://doi.org/10.5194/bg-2020-289
Preprint. Discussion started: 26 August 2020

Gradients of LMA with tree height are a result from leaf adaptation to changing light conditions and have previously been reported by multiple studies (Konôpka et al., 2016; Marshall and Monserud, 2003; Merilo et al., 2009; Morecroft and Roberts, 1999; Stancioiu and O'Hara, 2006; Xiao et al., 2006). Leaves exposed to intense sunlight in tree canopies tend to grow thicker and denser thereby accumulate more photosynthesizing biomass per unit surface area (Niinemets et al., 2001; Sonnewald, 2013). It is thus likely that foliar Hg content per gram dry weight is diluted in sun exposed canopy leaves relative to lower growing shade leaves explaining the observed gradient in foliar Hg concentrations with tree height (Fig. 5a). Foliar Hg content normalized to leaf area (ng Hg m^{-2}_{leaf}; Fig. 5c) is derived from the multiplication of Hg concentrations and respective LMA. As the gradient of LMA values with height (Fig. 5b) is reversed to and steeper than the gradient in Hg concentrations with height (Fig. 5a), foliar Hg content per leaf area (Fig. 5c) decreases from top to ground level. Therefore, care has to be taken when comparing different data sets of foliar Hg concentrations as foliar Hg concentrations depend on leaf morphology which varies with height and between tree species.

3.3 Effect of crown height on foliar Hg uptake rates per leaf area

Hg uptake rates per leaf area ($upkateR_{leaf\ area}$) were higher in top canopy compared to mid canopy/ground level by a ratio of 2.19 for beech, 1.22 for oak and 1.72 for spruce. Thus, foliage takes up more Hg per area at top canopy level than at ground level (Fig. 6a exemplary for beech). We propose two mechanisms that possibly explain increasing Hg uptake rates per leaf area with crown height: **(1) Vertical variation in stomatal density and stomatal conductance:** Leaves from the top of the canopy (sun leaves) have been reported to exhibit a significantly higher mean stomatal density than leaves within the canopy (shade leaves) (Poole et al., 1996). A higher stomatal density (number of stomata pores per unit leaf area) is associated with a higher Hg content per leaf area (Laacouri et al., 2013). The observed gradient of higher Hg uptake per leaf area towards the top canopy (Fig. 6a) possibly reflects higher stomatal density in sun leaves compared to shade leaves at ground level. Supplementary to stomatal density, we hypothesize that stomatal conductance to water vapor is a defining parameter for foliar Hg uptake per area. We measured stomatal conductance under dry conditions at Hölstein at noon on 17 July 2019 and observed higher average values in top canopy beech leaves than in ground level beech leaves (Fig. 6b). Stomatal conductance to water vapor is subject to temporal change depending on meteorological conditions and soil moisture content (Körner, 2013; Schulze, 1986). Nevertheless, the observed gradient in stomatal conductance with tree height (Fig. 6b) conceivably indicates that foliar-atmosphere exchange of water vapor and Hg(0) are related. (**2) Vertical air Hg(0) gradient:** We observed a small gradient in atmospheric Hg(0) from 1.6 ng m^{-3} at the top (35 m a.g.l) to 1.4 ± 0.08 ng m^{-3} at ground level (1.6 m a.g.l.) integrated over the growing season 2018 (May – October) and from 1.7 ng m^{-3} (35 m a.g.l) to 1.4 ng m^{-3} (1.6 m a.g.l.) integrated over the growing season 2019 (May – September) (Fig. 6c). We hypothesize that depletion in atmospheric Hg(0) within the canopy was driven by foliar uptake of atmospheric Hg(0) (Fu et al., 2016; Jiskra et al., 2019). The vertical Hg(0) gradient in air possibly contributed to the gradient of Hg content per leaf area in beech, oak and spruce from top canopy to ground/mid canopy because ground level leaf area intercepts less air Hg(0) than canopy leaf area. A caveat to consider is that the Hg(0) concentration gradient measured depends on sampling rates of deployed passive samplers, which were considered to be constant with height (detailed discussion in S7).

https://doi.org/10.5194/bg-2020-289
Preprint. Discussion started: 26 August 2020

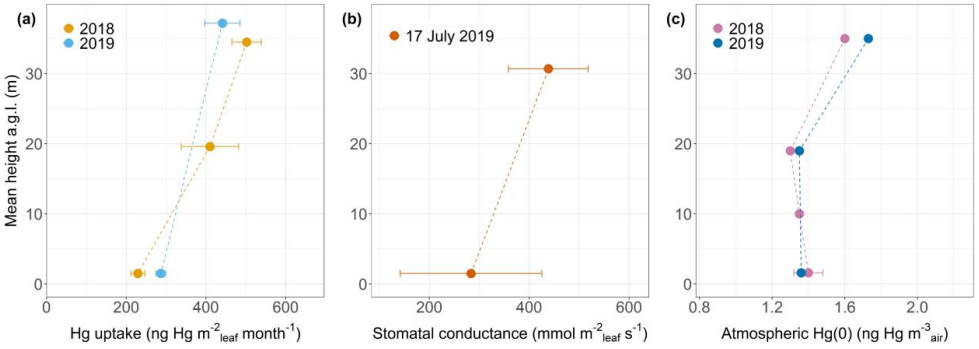

Fig. 6: (a) foliar Hg uptake rate per leaf area (ng Hg m^{-2}_{leaf} $month^{-1}$; linear regression coefficient ± se) by beech leaves at various tree heights (m) at Hölstein during two growing seasons 2018 and 2019; (b) Stomatal conductance to water vapor (mmol m^{-2}_{leaf} s^{-1}; mean ± sd) measured in Hölstein beech leaves at top canopy and ground level under dry conditions at noon on 17 July 2019; (c) Atmospheric Hg(0) (ng Hg m^{-3}_{air}) at various heights in Hölstein measured with passive air samplers and integrated over the 2018 and 2019 growing season respectively. Error bars at ground level height (1.6 m) of 2018 data denote one standard deviation between 4 passive samplers.

Re-emission of Hg(0) from foliage driven by photoreduction of Hg(II) to Hg(0) can counterbalance gross uptake of Hg(0) (Yuan et al., 2019). Re-emission rates will be enhanced in the top of the canopy due to higher light availability. However, re-emission rates were not large enough to compensate for higher Hg uptake per leaf area by top canopy leaves compared to ground level leaves (Fig. 6a).

3.4 Effect of tree functional group (deciduous vs. conifer) on foliar Hg uptake

Broad leaves of deciduous species (beech and oak) in Hölstein exhibited on average approximately five times higher Hg concentration increases (5.3 ± 0.6 ng Hg g^{-1} d.w. $month^{-1}$; mean ± se) compared to current-season pine and spruce needles (mean: 1.1 ± 0.4 ng Hg g^{-1} d.w. $month^{-1}$; mean ± se) (Fig. 7a). Higher Hg concentrations in broad leaves directly compared to conifer needles were also found by Blackwell and Driscoll (2015); Navrátil et al. (2016) but not by Hall and St. Louis (2004); Obrist et al. (2011, 2012). Foliar Hg uptake rates normalized to leaf area in Hölstein were approximately 3 times higher in broad leaves (622 ± 84 ng Hg m^{-2}_{leaf} $month^{-1}$; mean ± se) than in conifer needles (222 ± 81 ng Hg m^{-2}_{leaf} $month^{-1}$; mean ± se) (Fig. 7b). Thus, our results exhibit higher foliar Hg uptake per leaf area in broad leaves than in current-season conifer needles.

https://doi.org/10.5194/bg-2020-289
Preprint. Discussion started: 26 August 2020

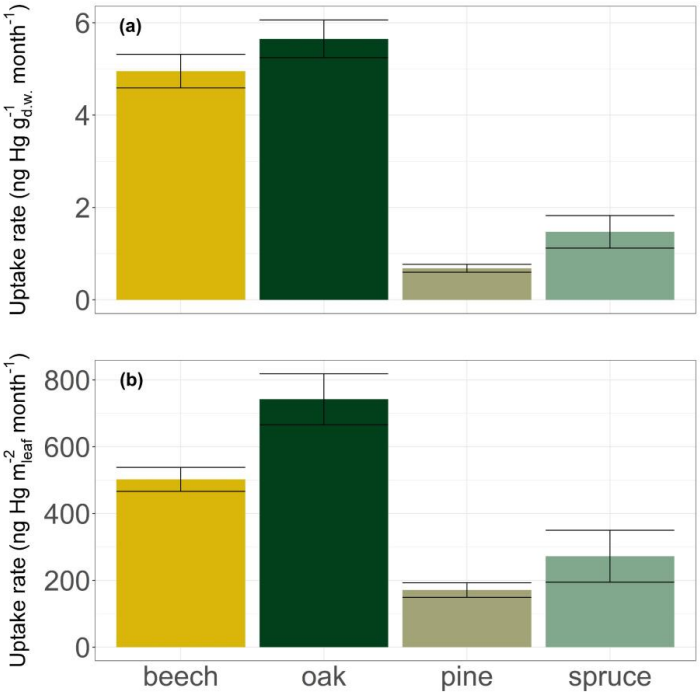

Fig. 7: Uptake rates by leaves and current-season needles of 4 tree species at Hölstein (a) of ng Hg g^{-1} foliage dry weight and month; (b) of Hg uptake rate normalized to leaf area in ng Hg m^{-2} $month^{-1}$. Error bars denote standard errors of the linear regression of foliar Hg concentrations over the growing season.

We propose that Hg uptake rates have to be assessed in the context of different physiological characteristics of conifer needles and broad leaves. Needles generally have a larger LMA (245 ± 62 g m^{-2} in Hölstein) than broad leaves (79 ± 38 g m^{-2} in Hölstein). Plant tissues with large LMA such as needles are associated with low metabolic activity including photosynthesis and respiration (Körner, 2013; Reich et al., 1997; Wright et al., 2004). Accordingly, the stomatal conductance to water vapor of canopy foliage in Hölstein on 17 July 2019 was lower for coniferous pine needles (289 ± 137 mmol m^{-2} s^{-1}; mean ± sd; n = 14) than for broad leaves of beech (438 ± 80 mmol m^{-2} s^{-1}; mean ± sd; n = 14) and oak (849 ± 221 mmol m^{-2} s^{-1}; mean ± sd; n = 15). The variation between foliage functional groups (conifer needles vs. broad leaves) indicates that foliar Hg uptake is related to stomatal conductance.

3.5 Foliar Hg uptake fluxes per ground area

We calculated foliar Hg uptake fluxes per ground area (m^2_{ground}) by multiplying foliar Hg uptake rates per leaf area (m^2_{leaf}) with species-specific LAI (Eq. 1). LAI values (mean ± sd) differed between tree species and were highest in spruce (7.3 ± 2.1) and beech (7.0 ± 1.6) and lowest in pine (2.9 ± 1.4) and birch (2.6 ± 1.2) (Table S2). In general, forests consisting of spruce trees with high LAI might therefore exhibit higher Hg uptake fluxes than deciduous forests with low average LAI even though Hg uptake rates per leaf area might be lower for conifer needles than for broad leaves (Sect. 3.4). We applied correction factors for needle age for conifer samples (Eq. 4) and crown height for sites where we collected top canopy samples (Hölstein, Hyltemossa, Norunda and Svartberget) (Eq. 6). The foliar Hg uptake flux showed a large variation ranging from 2 µg Hg m^{-2} (Pallas, pine) to 26 µg Hg m^{-2} (Schauinsland, beech) over the 2018 growing season (Fig. S6). The 4 sites where samples were

https://doi.org/10.5194/bg-2020-289
Preprint. Discussion started: 26 August 2020

collected from top canopy exhibited a smaller range for spruce between sites from 7 to 15 µg Hg m^{-2} $season^{-1}$ (Fig. 8). Given the systematic variation of Hg uptake rates with tree height (Fig. 5) we cannot exclude that the inconsistent sampling strategy might have influenced the observed Hg uptake fluxes among the 10 sampling sites. We will therefore not further discuss the observed variation between sites. To scale up site-based Hg uptake fluxes, we only consider sites where we consistently sampled the top third of the canopy (Hölstein, Hyltemossa, Norunda and Svartberget). The average foliar Hg uptake fluxes of each species at the four crown sampling sites (mean ± se between sites) during the 2018 growing season was 18 ± 3 µg Hg m^{-2} for beech, 26 ± 5 µg Hg m^{-2} for oak, 4 ± 1 µg Hg m^{-2} for pine and 11 ± 1 µg Hg m^{-2} for spruce (see S13 for standard errors of fluxes). Deciduous trees exhibited higher foliar uptake fluxes compared to coniferous trees resulting from generally higher uptake rates per leaf area (Fig. 7b) owing to higher physiological activity of deciduous trees.

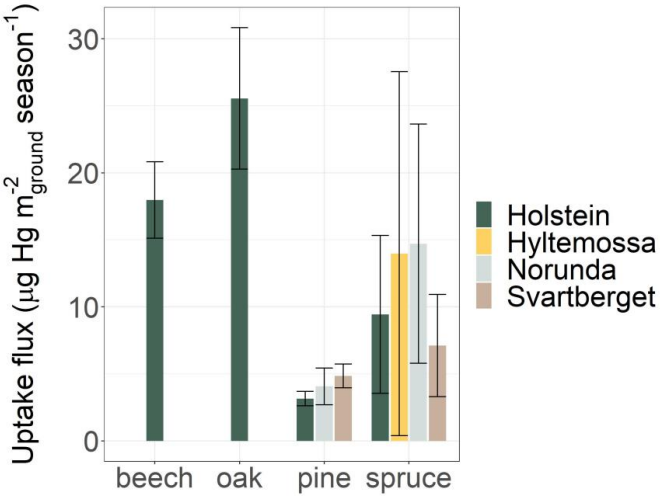

Fig. 8: Foliar Hg uptake fluxes (µg Hg m^{-2} during the 2018 growing season) at four forested research sites where foliage samples were taken from crown height. Error bars indicate one standard error of the regression slope.

3.6 Foliar Hg uptake fluxes along a latitudinal gradient in Europe

We calculated total Hg uptake fluxes at each research site as the sum of Hg uptake fluxes of each tree species and research site weighted by the relative abundance of the respective tree species to the other examined tree species at each site (Fig. 9). The average foliar Hg uptake flux of the 4 research sites where foliage samples were obtained from tree crown heights over the 2018 growing season was 11 ± 3 µg Hg m^{-2} (mean ± sd). Spruce needle Hg uptake fluxes did not exhibit a clear trend with latitude (Fig. 8b with sites sorted for latitude).

The aboveground foliar Hg uptake fluxes per site (range 6 - 14 µg Hg m^{-2} growing $season^{-1}$) are in the lower range of published Hg litterfall fluxes in Europe and North America measured for various years, which range from 9.7 to 28.5 µg Hg m^{-2} y^{-1} (Demers et al., 2007; Juillerat et al., 2012; Navrátil et al., 2016; Rea et al., 1996, 2002; Risch et al., 2012, 2017).

The average wet Hg(II) deposition fluxes measured at Schauinsland, Schmücke, Råö, Bredkälen and Pallas over the course of the sampling period was 2.3 ± 0.3 µg Hg m^{-2} (mean ± sd). Wet Hg deposition fluxes were consistently

https://doi.org/10.5194/bg-2020-289
Preprint. Discussion started: 26 August 2020

lower than foliar Hg uptake fluxes. Our data constrain that foliar Hg uptake is a major deposition pathway to terrestrial surfaces in Europe, exceeding direct wet deposition of Hg(II) by a factor of four. Note that this assessment only compares Hg(0) uptake by foliage and does not take into account Hg incorporated into wood biomass (Navrátil et al., 2019) or Hg(0) adsorbed to leaf surfaces that is washed off between sampling events as throughfall (Demers et al., 2007; Rea et al., 1996, 2001). Total Hg(0) deposition fluxes to terrestrial ecosystems, which also include Hg(0) deposition to soils and litter (Obrist et al., 2014, 2017; Pokharel and Obrist, 2011; Zhang et al., 2009) are therefore expected to be higher than foliar uptake fluxes quantified here.

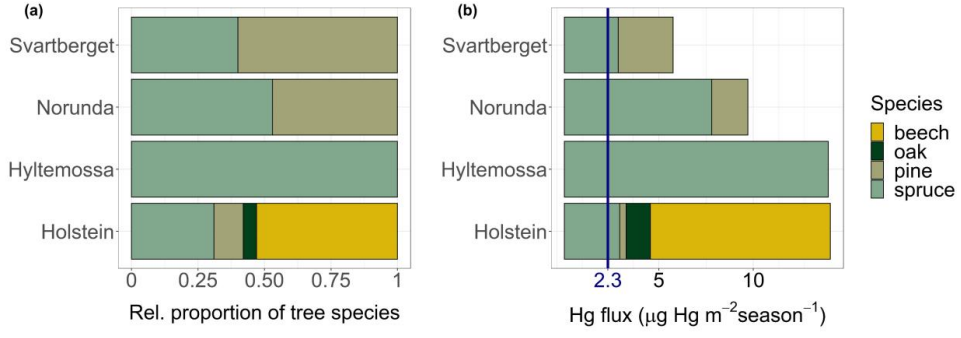

Fig. 9: (a) Relative proportion of tree species to each other and (b) foliar Hg fluxes (µg Hg m^{-2} over the 2018 growing season) at 4 European research sites ordered by latitude from South (Hölstein at 47° N) to North (Svartberget at 64° N); blue label of 2.3 µg Hg m^{-2} $season^{-1}$ corresponds to the average wet deposition flux measured at 5 sites over the course of the sampling period

Averaging species-specific foliar Hg uptake fluxes and weighting them with the tree species proportion in Europe derived from Brus et al. (2012) yields an average foliar Hg uptake flux for Europe of 10.4 ± 2 µg Hg m^{-2} over the 2018 growing season (weighted mean ± se). Extrapolation of this weighted mean to the land area of European forests (192.672 × 10^6 hectares) results in a foliar flux of 20 ± 3 Mg Hg during the 2018 growing season (see Sect. S12 for details on flux extrapolation and Sect. S13 for error propagation). Under the assumption that tree species in the global temperate zone are distributed equally to tree species in Europe we estimated an approximate foliar flux of 108 ± 18 Mg Hg to the area of global temperate forests (1.04 * 10^9 hectares) (Tyrrell et al., 2012) during the 2018 growing season. This global extrapolation is at the lower end of global Hg litterfall deposition flux (163 Mg Hg yr^{-1}) estimated for temperate forests based on a Hg litterfall flux database of measurements between 1995 – 2015 (Wang et al., 2016). In order to obtain a more precise foliar Hg uptake flux estimate to European and global forests, improved spatially resolved foliar Hg data and comprehensive ground-based forest statistics of tree species composition are needed.

4. Conclusion

We observed that Hg concentrations in foliage increased over the growing season in broadleaf and coniferous trees. Concentrations of Hg in multi-year needles increased with age. The foliar Hg uptake normalized to leaf area was higher on top of the canopy than at ground level. The temporal and vertical variation of foliar Hg uptake fluxes are consistent with the notion that stomatal uptake represents the main deposition pathway to atmospheric Hg(0). We emphasize that standardized sampling strategies and reporting of sampling height and needle age class is essential to allow for comparison of foliar Hg results between different studies.

https://doi.org/10.5194/bg-2020-289
Preprint. Discussion started: 26 August 2020

We developed a bottom-up approach to quantify foliar Hg(0) uptake fluxes on an ecosystem scale, considering the systematic variations in crown height, needle age and tree species. Our bottom-up approach integrates aboveground foliar Hg(0) uptake rates over the entire growing season and the whole tree level. We thus suggest that our approach provides a robust method to assess foliar Hg(0) uptake fluxes on a species level as well as on an ecosystem scale at a high temporal resolution. This approach is complementary to litterfall mass balances approaches, which provide Hg deposition estimates integrated over an entire year. We suspect that the foliar Hg uptake fluxes measured in this study represent net Hg(0) uptake fluxes as the increase of foliar Hg concentration was linear with time which would include possible Hg(0) re-emission from foliage (Yuan et al., 2019). With the bottom-up approach presented here, it is thus possible to obtain net foliar Hg(0) uptake fluxes that are temporally resolved over the growing season depending on the number of temporal foliar Hg measurements. The linear uptake of Hg(0) observed in this study across 10 European sites and for 6 different species suggests that forest foliage take up Hg(0) from the atmosphere over the entire growing season, supporting the notion that foliar uptake of Hg(0) drives the seasonal depletion in atmospheric Hg(0) in the Northern Hemisphere (Jiskra et al., 2018).

Our study demonstrates that foliar Hg uptake is an important deposition pathway to terrestrial surfaces and exceeds wet deposition by a factor of 4 on average. In contrast to Hg(II) in wet deposition, which is monitored in atmospheric deposition networks (EMEP, 2016; Pacyna et al., 2009), there is no standardized and established program to monitor Hg deposition in foliage or litterfall across Europe. We call for including foliar mercury deposition in monitoring networks on a country and international level. Robust and standardized data on the development of Hg deposition to foliage and forest ecosystems will allow to assess the effectiveness of the Minamata convention on mercury (Minamata Convention, 2019) and impact of climate change on mercury deposition to terrestrial ecosystems in the future.

Author contribution

M.J. designed the study. L.W. and C.J. carried out the field sampling and analytical measurements. L.W. performed the data analysis. S.O. and G.H. gave experimental advice and sampling support. C.A. and A.K. provided feedback and research infrastructure. L.W. wrote the manuscript in consultation with M.J. All authors discussed the manuscript and provided comments.

Acknowledgment

We are grateful to Fabienne Bracher, Emanuel Glauser and Judith Kobler Waldis for their help with foliage sample preparation and analysis. We acknowledge the Swiss Canopy Crane II (SCCII) Site at Hölstein operated by the Physiological Plant Ecology Research Group at the University of Basel and thank André Kühne and Matthias Arend for their on-site support. We thank Frank Wania from the University of Toronto for contributing valuable mercury passive air samplers and activated carbon. Hans-Peter Dietrich and Stephan Raspe from the Bavarian State Institute of Forestry thankfully provided us with multi-year foliage samples from Bavaria. We acknowledge ICOS Sweden for providing data from Hyltemossa, Norunda and Svartberget and we would like to thank Irene Lehner, Tobias Biermann, Michal Heliasz, Antonin Kusbach, Johan Ahlgren, Ulla Nylander, Mikael Holmlund, Pernilla Löfvenius and Per Marklund for assistance in foliage sampling and experimental support. Volkmar Timmermann and Helge Meissner from NIBIO gratefully organized and performed foliage sampling at Hurdal. We thank Elke Bieber, Frank Meinhardt and Rita Junek from the German Federal Environment Agency for their support at Schauinsland and Schmücke air monitoring sites. We are grateful to Michelle Nerentorp Mastromonaco and Ingvar Wängberg from IVL and Eva-Britt Edin for foliage sampling support and site access at Råö and

https://doi.org/10.5194/bg-2020-289
Preprint. Discussion started: 26 August 2020

Bredkälen. We thank Katriina Kyllönen from FMI and Valtteri Hyöky for foliage sampling assistance and site access at Pallas. Special thanks go to Jann Launer for drawing Fig. 2. Finally, we thank Christian Körner for his helpful answers to questions on plant physiology.

Financial support

The work of this paper was funded by the Swiss National Science Foundation (SNSF) project 174101. The crane at the SCCII Site is funded by the Swiss Federal Office for the Environment (FOEN). The Swedish research infrastructures, ICOS and SITES, are both financed by the Swedish Research Council and partner universities.

Data availability

Foliar Hg uptake fluxes at all sites are given in the Supporting Information. Hg concentrations, metadata of all foliage samples collected in this study are accessible at https://zenodo.org/record/3957873#.XxmttOfRabh

Competing interests

The authors declare that they have no conflict of interest.

References

Ariya, P. A., Amyot, M., Dastoor, A., Deeds, D., Feinberg, A., Kos, G., Poulain, A., Ryjkov, A., Semeniuk, K., Subir, M. and Toyota, K.: Mercury physicochemical and biogeochemical transformation in the atmosphere and at atmospheric interfaces: a review and future directions, Chem. Rev., 115(10), 3760–3802, doi:10.1021/cr500667e, 2015.

Assad, M., Parelle, J., Cazaux, D., Gimbert, F., Chalot, M. and Tatin-Froux, F.: Mercury uptake into poplar leaves, Chemosphere, 146, 1–7, doi:10.1016/j.chemosphere.2015.11.103, 2016.

Bishop, K., Shanley, J. B., Riscassi, A., de Wit, H. A., Eklöf, K., Meng, B., Mitchell, C., Osterwalder, S., Schuster, P. F., Webster, J. and Zhu, W.: Recent advances in understanding and measurement of mercury in the environment: Terrestrial Hg cycling, Sci. Total Environ., 721, 137647, doi:10.1016/j.scitotenv.2020.137647, 2020.

Blackwell, B. D. and Driscoll, C. T.: Using foliar and forest floor mercury concentrations to assess spatial patterns of mercury deposition, Environ. Pollut., 202, 126–134, doi:10.1016/j.envpol.2015.02.036, 2015.

Blackwell, B. D., Driscoll, C. T., Maxwell, J. A. and Holsen, T. M.: Changing climate alters inputs and pathways of mercury deposition to forested ecosystems, Biogeochemistry, 119(1–3), 215–228, doi:10.1007/s10533-014-9961-6, 2014.

Brus, D. J., Hengeveld, G. M., Walvoort, D. J. J., Goedhart, P. W., Heidema, A. H., Nabuurs, G. J. and Gunia, K.: Statistical mapping of tree species over Europe, European Journal of Forest Research, 131(1), 145–157, doi:10.1007/s10342-011-0513-5, 2012.

Burkhardt, J. and Pariyar, S.: Particulate pollutants are capable to "degrade" epicuticular waxes and to decrease the drought tolerance of Scots pine (Pinus sylvestris L.), Environ. Pollut., 184, 659–667, doi:10.1016/j.envpol.2013.04.041, 2014.

Bushey, J. T., Nallana, A. G., Montesdeoca, M. R. and Driscoll, C. T.: Mercury dynamics of a northern hardwood canopy, Atmos. Environ., 42(29), 6905–6914, doi:10.1016/j.atmosenv.2008.05.043, 2008.

539 Demers, J. D., Driscoll, C. T., Fahey, T. J. and Yavitt, J. B.: Mercury cycling in litter and soil in
540 different forest types in the Adirondack Region, New York, USA, Ecol. Appl., 17(5), 1341–1351,
541 doi:10.1890/06-1697.1, 2007.

542 Demers, J. D., Blum, J. D. and Zak, D. R.: Mercury isotopes in a forested ecosystem: Implications for
543 air-surface exchange dynamics and the global mercury cycle, Global Biogeochemical Cycles, 27(1),
544 222–238, doi:10.1002/gbc.20021, 2013.

545 Driscoll, C. T., Mason, R. P., Chan, H. M., Jacob, D. J. and Pirrone, N.: Mercury as a global pollutant:
546 sources, pathways, and effects, Environ. Sci. Technol., 47(10), 4967–4983, doi:10.1021/es305071v,
547 2013.

548 EMEP: Air pollution trends in the EMEP region between 1990 and 2012, Joint Report, 2016.

549 Enrico, M., Roux, G. L., Marusczak, N., Heimbürger, L.-E., Claustres, A., Fu, X., Sun, R. and Sonke,
550 J. E.: Atmospheric mercury transfer to peat bogs dominated by gaseous elemental mercury dry
551 deposition, Environ. Sci. Technol., 50(5), 2405–2412, doi:10.1021/acs.est.5b06058, 2016.

552 Ericksen, J. A. and Gustin, M. S.: Foliar exchange of mercury as a function of soil and air mercury
553 concentrations, Sci. Total Environ., 324(1), 271–279, doi:10.1016/j.scitotenv.2003.10.034, 2004.

554 EU: European Commission, 2011/833/EU: Commission Decision of 12 December 2011 on the reuse
555 of Commission documents, [online] Available from: https://eur-lex.europa.eu/eli/dec/2011/833/oj,
556 2011.

557 Fichtner, A., Sturm, K., Rickert, C., von Oheimb, G. and Härdtle, W.: Crown size-growth
558 relationships of European beech (Fagus sylvatica L.) are driven by the interplay of disturbance
559 intensity and inter-specific competition, Forest Ecol. Manag., 302, 178–184,
560 doi:10.1016/j.foreco.2013.03.027, 2013.

561 Fleck, J. A., Grigal, D. F. and Nater, E. A.: Mercury uptake by trees: an observational experiment,
562 Water Air Soil Poll., 115(1), 513–523, doi:10.1023/A:1005194608598, 1999.

563 Freeland, R. O.: Effect of age of leaves upon the rate of photosynthesis in some conifers, Plant
564 Physiol., 27(4), 685–690, doi:10.1104/pp.27.4.685, 1952.

565 Frescholtz, T. F., Gustin, M. S., Schorran, D. E. and Fernandez, G. C. J.: Assessing the source of
566 mercury in foliar tissue of quaking aspen, Environ. Toxicol. Chem., 22(9), 2114–2119,
567 doi:10.1002/etc.5620220922, 2003.

568 Fu, X., Zhu, W., Zhang, H., Sommar, J., Yu, B., Yang, X., Wang, X., Lin, C.-J. and Feng, X.:
569 Depletion of atmospheric gaseous elemental mercury by plant uptake at Mt. Changbai, Northeast
570 China, Atmos. Chem. Phys., 16(20), 12861–12873, doi:10.5194/acp-16-12861-2016, 2016.

571 Garonna, I., Jong, R. de, Wit, A. J. W. de, Mücher, C. A., Schmid, B. and Schaepman, M. E.: Strong
572 contribution of autumn phenology to changes in satellite-derived growing season length estimates
573 across Europe (1982–2011), Glob. Change Biol., 20(11), 3457–3470, doi:10.1111/gcb.12625, 2014.

574 Gencarelli, C. N., De Simone, F., Hedgecock, I. M., Sprovieri, F., Yang, X. and Pirrone, N.: European
575 and Mediterranean mercury modelling: Local and long-range contributions to the deposition flux,
576 Atmos. Environ., 117, 162–168, doi:10.1016/j.atmosenv.2015.07.015, 2015.

577 Graydon, J. A., St. Louis, V. L., Lindberg, S. E., Hintelmann, H. and Krabbenhoft, D. P.:
578 Investigation of mercury exchange between forest canopy vegetation and the atmosphere using a new
579 dynamic chamber, Environ. Sci. Technol., 40(15), 4680–4688, doi:10.1021/es0604616, 2006.

580 Grigal, D. F.: Inputs and outputs of mercury from terrestrial watersheds: a review, Environ. Rev.,
581 10(1), 1–39, 2002.

https://doi.org/10.5194/bg-2020-289
Preprint. Discussion started: 26 August 2020

582 Güney, A., Zimmermann, R., Krupp, A. and Haas, K.: Needle characteristics of Lebanon cedar
583 (Cedrus libani A.Rich.): degradation of epicuticular waxes and decrease of photosynthetic rates with
584 increasing needle age, Turk. J. Agric. For., 40, 386–396, doi:10.3906/tar-1507-63, 2016.

585 Hakkila, P.: Hakkuupoistuman Latvusmassa: Crown mass of trees at the harvesting phase, The
586 Finnish Forest Research Institute, 1991.

587 Hall, B. D. and St. Louis, V. L.: Methylmercury and Total Mercury in Plant Litter Decomposing in
588 Upland Forests and Flooded Landscapes, Environ. Sci. Technol., 38(19), 5010–5021,
589 doi:10.1021/es049800q, 2004.

590 Hirose, T.: Development of the Monsi-Saeki Theory on Canopy Structure and Function, Ann. Bot.,
591 95(3), 483–494, doi:10.1093/aob/mci047, 2004.

592 Hutnik, R. J., McClenahen, J. R., Long, R. P. and Davis, D. D.: Mercury Accumulation in Pinus nigra
593 (Austrian Pine), Northeast. Nat., 21(4), 529–540, doi:10.1656/045.021.0402, 2014.

594 Iio, A. and Ito, A.: A global database of field-observed leaf area index in woody plant species, 1932 -
595 2011. Data set available online from Oak Ridge National Laboratory Distributed Active Archive
596 Center, Oak Ridge, Tennessee, USA, Oak Ridge, doi:https://daac.ornl.gov/cgi-
597 bin/dsviewer.pl?ds_id=1231, 2014.

598 Jaffe, D. A., Lyman, S., Amos, H. M., Gustin, M. S., Huang, J., Selin, N. E., Levin, L., ter Schure, A.,
599 Mason, R. P., Talbot, R., Rutter, A., Finley, B., Jaeglé, L., Shah, V., McClure, C., Ambrose, J., Gratz,
600 L., Lindberg, S., Weiss-Penzias, P., Sheu, G.-R., Feddersen, D., Horvat, M., Dastoor, A., Hynes, A. J.,
601 Mao, H., Sonke, J. E., Slemr, F., Fisher, J. A., Ebinghaus, R., Zhang, Y. and Edwards, G.: Progress on
602 understanding atmospheric mercury hampered by uncertain measurements, Environ. Sci. Technol.,
603 48(13), 7204–7206, doi:10.1021/es5026432, 2014.

604 Jensen, A. M., Warren, J. M., Hanson, P. J., Childs, J. and Wullschleger, S. D.: Needle age and season
605 influence photosynthetic temperature response and total annual carbon uptake in mature Picea
606 mariana trees, Ann. Bot., 116(5), 821–832, doi:10.1093/aob/mcv115, 2015.

607 Jiskra, M., Wiederhold, J. G., Skyllberg, U., Kronberg, R.-M., Hajdas, I. and Kretzschmar, R.:
608 Mercury deposition and re-emission pathways in boreal forest soils investigated with Hg isotope
609 signatures, Environ. Sci. Technol., 49(12), 7188–7196, 2015.

610 Jiskra, M., Sonke, J. E., Obrist, D., Bieser, J., Ebinghaus, R., Myhre, C. L., Pfaffhuber, K. A.,
611 Wängberg, I., Kyllönen, K., Worthy, D., Martin, L. G., Labuschagne, C., Mkololo, T., Ramonet, M.,
612 Magand, O. and Dommergue, A.: A vegetation control on seasonal variations in global atmospheric
613 mercury concentrations, Nat. Geosci., 1–7, doi:10.1038/s41561-018-0078-8, 2018.

614 Jiskra, M., Sonke, J. E., Agnan, Y., Helmig, D. and Obrist, D.: Insights from mercury stable isotopes
615 on terrestrial–atmosphere exchange of Hg(0) in the Arctic tundra, Biogeosciences, 16(20), 4051–
616 4064, doi:10.5194/bg-16-4051-2019, 2019.

617 JRC: European Commission, Joint Research Centre (JRC): Forest Type Map 2006., [online] Available
618 from: https://forest.jrc.ec.europa.eu/en/past-activities/forest-mapping/#Downloadforestmaps, 2010.

619 Juillerat, J. I., Ross, D. S. and Bank, M. S.: Mercury in litterfall and upper soil horizons in forested
620 ecosystems in Vermont, USA, Environ. Toxicol. Chem., 31(8), 1720–1729, doi:10.1002/etc.1896,
621 2012.

622 Kahmen, A., Lustenberger, S., Zemp, E. and Erny, B.: The Swiss Canopy Crane Experiment II and
623 the botanical garden (University Basel), DBG [online] Available from:
624 https://www.dbges.de/de/system/files/Tagung_Bern/Exkursionen/g_08_final_0.pdf, 2019.

https://doi.org/10.5194/bg-2020-289
Preprint. Discussion started: 26 August 2020

625 Kempeneers, P., Sedano, F., Seebach, L., Strobl, P. and San-Miguel-Ayanz, J.: Data fusion of
626 different spatial resolution remote sensing images applied to forest-type mapping, IEEE Transactions
627 on Geoscience and Remote Sensing, 49(12), 4977–4986, doi:10.1109/TGRS.2011.2158548, 2011.

628 Konôpka, B., Pajtík, J., Marušák, R., Bošeľa, M. and Lukac, M.: Specific leaf area and leaf area index
629 in developing stands of Fagus sylvatica L. and Picea abies Karst., Forest Ecol. Manag., 364, 52–59,
630 doi:10.1016/j.foreco.2015.12.005, 2016.

631 Körner, C.: Plant–Environment Interactions, in Strasburger's Plant Sciences: Including Prokaryotes
632 and Fungi, edited by A. Bresinsky, C. Körner, J. W. Kadereit, G. Neuhaus, and U. Sonnewald, pp.
633 1065–1166, Springer, Berlin, Heidelberg., 2013.

634 Laacouri, A., Nater, E. A. and Kolka, R. K.: Distribution and uptake dynamics of mercury in leaves of
635 common deciduous tree species in Minnesota, U.S.A., Environ. Sci. Technol., 47(18), 10462–10470,
636 doi:10.1021/es401357z, 2013.

637 Lange, H.: Carbon exchange measurements at a flux tower in Hurdal, SNS Efinord Growth and Yield
638 Network Conference NIBIO Bok, 3, 2017.

639 Lindroth, A., Heliasz, M., Klemedtsson, L., Friborg, T., Nilsson, M., Löfvenius, O., Rutgersson, A.
640 and Stiegler, C.: ICOS Sweden - a national infrastructure network for greenhouse gas research, EGU
641 Geophysical Research Abstracts, 17, 2015.

642 Lindroth, A., Holst, J., Heliasz, M., Vestin, P., Lagergren, F., Biermann, T., Cai, Z. and Mölder, M.:
643 Effects of low thinning on carbon dioxide fluxes in a mixed hemiboreal forest, Agr. Forest Meteorol.,
644 262, 59–70, doi:10.1016/j.agrformet.2018.06.021, 2018.

645 Lodenius, M., Tulisalo, E. and Soltanpour-Gargari, A.: Exchange of mercury between atmosphere and
646 vegetation under contaminated conditions, Sci. Total Environ., 304(1), 169–174, doi:10.1016/S0048-
647 9697(02)00566-1, 2003.

648 Lohila, A., Penttilä, T., Jortikka, S., Aalto, T., Anttila, P., Asmi, E., Aurela, M., Hatakka, J., Hellén,
649 H., Henttonen, H., Hänninen, P., Kilkki, J., Kyllönen, K., Laurila, T., Lepistö, A., Lihavainen, H.,
650 Makkonen, U., Paatero, J., Rask, M., Sutinen, R., Tuovinen, J.-P., Vuorenmaa, J. and Viisanen, Y.:
651 Preface to the special issue on integrated research of atmosphere, ecosystems and environment at
652 Pallas, Boreal Environ. Res., 20, 431–454, 2015.

653 Loustau, D., Altimir, N., Barbaste, M., Gielen, B., Jiménez, S. M., Klumpp, K., Linder, S., Matteucci,
654 G., Merbold, L., Op de Beeck, M., Soulé, P., Thimonier, A., Vincke, C. and Waldner, P.: Sampling
655 and collecting foliage elements for the determination of the foliar nutrients in ICOS ecosystem
656 stations, Int. Agrophys., 32, 665–676, doi:doi: 10.1515/intag-2017-0038, 2018.

657 Manceau, A., Wang, J., Rovezzi, M., Glatzel, P. and Feng, X.: Biogenesis of mercury–sulfur
658 nanoparticles in plant leaves from atmospheric gaseous mercury, Environ. Sci. Technol., 52(7), 3935–
659 3948, doi:10.1021/acs.est.7b05452, 2018.

660 Marshall, J. D. and Monserud, R. A.: Foliage height influences specific leaf area of three conifer
661 species, Can. J. For. Res., 33(1), 164–170, doi:10.1139/x02-158, 2003.

662 Matyssek, R., Reich, P., Oren, R. and Winner, W. E.: 9 - Response Mechanisms of Conifers to Air
663 Pollutants, in Ecophysiology of Coniferous Forests, edited by W. K. Smith and T. M. Hinckley, pp.
664 255–308, Academic Press, San Diego., 1995.

665 McLagan, D. S., Mitchell, C. P. J., Huang, H., Lei, Y. D., Cole, A. S., Steffen, A., Hung, H. and
666 Wania, F.: A high-precision passive air sampler for gaseous mercury, Environ. Sci. Technol. Lett.,
667 3(1), 24–29, doi:10.1021/acs.estlett.5b00319, 2016.

https://doi.org/10.5194/bg-2020-289
Preprint. Discussion started: 26 August 2020

668 Merilo, E., Tulva, I., Räim, O., Kükit, A., Sellin, A. and Kull, O.: Changes in needle nitrogen
669 partitioning and photosynthesis during 80 years of tree ontogeny in Picea abies, Trees, 23(5), 951–
670 958, doi:10.1007/s00468-009-0337-9, 2009.

671 Millhollen, A. G., Gustin, M. S. and Obrist, D.: Foliar mercury accumulation and exchange for three
672 tree species, Environ. Sci. Technol., 40(19), 6001–6006, doi:10.1021/es0609194, 2006.

673 Minamata Convention: DRAFT Report on the work of the ad hoc technical group on effectiveness
674 evaluation, ,
675 doi:http://www.mercuryconvention.org/Portals/11/documents/meetings/COP3/Effectiveness/EU-
676 experts-comments-04Sep2019.pdf, 2019.

677 Monsi, M. and Saeki, T.: On the factor light in plant communities and its importance for matter
678 production, Ann. Bot., 95(3), 549–567, doi:10.1093/aob/mci052, 2004.

679 Morecroft, M. D. and Roberts, J. M.: Photosynthesis and stomatal conductance of mature canopy oak
680 (Quercus robur) and sycamore (Acer pseudoplatanus) trees throughout the growing season, Funct.
681 Ecol., 13(3), 332–342, doi:10.1046/j.1365-2435.1999.00327.x, 1999.

682 Navrátil, T., Shanley, J. B., Rohovec, J., Oulehle, F., Šimeček, M., Houška, J. and Cudlín, P.: Soil
683 mercury distribution in adjacent coniferous and deciduous stands highly impacted by acid rain in the
684 Ore Mountains, Czech Republic, Appl. Geochem., 75, 63–75, doi:10.1016/j.apgeochem.2016.10.005,
685 2016.

686 Navrátil, T., Nováková, T., Roll, M., Shanley, J. B., Kopáček, J., Rohovec, J., Kaňa, J. and Cudlín, P.:
687 Decreasing litterfall mercury deposition in central European coniferous forests and effects of bark
688 beetle infestation, Sci. Total Environ., 682, 213–225, doi:10.1016/j.scitotenv.2019.05.093, 2019.

689 Niinemets, U., Ellsworth, D. S., Lukjanova, A. and Tobias, M.: Site fertility and the morphological
690 and photosynthetic acclimation of Pinus sylvestris needles to light, Tree Physiol., 21(17), 1231–1244,
691 doi:10.1093/treephys/21.17.1231, 2001.

692 Obrist, D.: Atmospheric mercury pollution due to losses of terrestrial carbon pools?,
693 Biogeochemistry, 85(2), 119–123, doi:10.1007/s10533-007-9108-0, 2007.

694 Obrist, D., Johnson, D. W., Lindberg, S. E., Luo, Y., Hararuk, O., Bracho, R., Battles, J. J., Dail, D.
695 B., Edmonds, R. L., Monson, R. K., Ollinger, S. V., Pallardy, S. G., Pregitzer, K. S. and Todd, D. E.:
696 Mercury distribution across 14 U.S. forests. Part I: spatial patterns of concentrations in biomass, litter,
697 and soils, Environ. Sci. Technol., 45(9), 3974–3981, doi:10.1021/es104384m, 2011.

698 Obrist, D., Johnson, D. W. and Edmonds, R. L.: Effects of vegetation type on mercury concentrations
699 and pools in two adjacent coniferous and deciduous forests, J. Plant. Nut. Soil Sc., 175(1), 68–77,
700 doi:10.1002/jpln.201000415, 2012.

701 Obrist, D., Pokharel, A. K. and Moore, C.: Vertical profile measurements of soil air suggest
702 immobilization of gaseous elemental mercury in mineral soil, Environ. Sci. Technol., 48(4), 2242–
703 2252, doi:10.1021/es4048297, 2014.

704 Obrist, D., Agnan, Y., Jiskra, M., Olson, C. L., Colegrove, D. P., Hueber, J., Moore, C. W., Sonke, J.
705 E. and Helmig, D.: Tundra uptake of atmospheric elemental mercury drives Arctic mercury pollution,
706 Nature, 547(7662), 201–204, doi:10.1038/nature22997, 2017.

707 Obrist, D., Kirk, J. L., Zhang, L., Sunderland, E. M., Jiskra, M. and Selin, N. E.: A review of global
708 environmental mercury processes in response to human and natural perturbations: Changes of
709 emissions, climate, and land use, Ambio, 47(2), 116–140, doi:10.1007/s13280-017-1004-9, 2018.

710 Ollerova, H., Maruskova, A., Kontrisova, O. and Pliestikova, L.: Mercury accumulation in Picea abies
711 (L.) Karst. needles with regard to needle age, Pol. J. Environ. Stud., 19(6), 1401–1404, 2010.

712 Op de Beeck, M., Gielen, B., Jonckheere, I., Samson, R., Janssens, I. A. and Ceulemans, R.: Needle
713 age-related and seasonal photosynthetic capacity variation is negligible for modelling yearly gas
714 exchange of a sparse temperate Scots pine forest, Biogeosciences, 7(1), 199–215, doi:10.5194/bg-7-
715 199-2010, 2010.

716 Pacyna, J. M., Pacyna, E. G. and Aas, W.: Changes of emissions and atmospheric deposition of
717 mercury, lead, and cadmium, Atmos. Environ., 43(1), 117–127, doi:10.1016/j.atmosenv.2008.09.066,
718 2009.

719 Pokharel, A. K. and Obrist, D.: Fate of mercury in tree litter during decomposition, Biogeosciences,
720 8(9), 2507–2521, doi:10.5194/bg-8-2507-2011, 2011.

721 Poole, I., Weyers, J. D. B., Lawson, T. and Raven, J. A.: Variations in stomatal density and index:
722 implications for palaeoclimatic reconstructions, Plant Cell Environ., 19(6), 705–712,
723 doi:10.1111/j.1365-3040.1996.tb00405.x, 1996.

724 Prestbo, E. M. and Gay, D. A.: Wet deposition of mercury in the U.S. and Canada, 1996–2005:
725 Results and analysis of the NADP mercury deposition network (MDN), Atmos. Environ., 43(27),
726 4223–4233, doi:10.1016/j.atmosenv.2009.05.028, 2009.

727 Rasmussen, P. E., Mierle, G. and Nriagu, J. O.: The analysis of vegetation for total mercury, Water
728 Air Soil Poll., 56(1), 379–390, doi:10.1007/BF00342285, 1991.

729 Rautio, P., Fürst, A., Stefan, K., Raitio, H. and Bartels, U.: UNECE ICP Forests Programme Co-
730 ordinating Centre (ed.): Manual on methods and criteria for harmonized sampling, assessment,
731 monitoring and analysis of the effects of air pollution on forests. Part XII: Sampling and analysis of
732 needles and leaves., Thünen Institute of Forest Ecosystems, Eberswalde, Germany, 2016.

733 Rea, A. W., Keeler, G. J. and Scherbatskoy, T.: The deposition of mercury in throughfall and litterfall
734 in the Lake Champlain Watershed: A short-term study, Atmos. Environ., 30(19), 3257–3263,
735 doi:10.1016/1352-2310(96)00087-8, 1996.

736 Rea, A. W., Lindberg, S. E. and Keeler, G. J.: Dry deposition and foliar leaching of mercury and
737 selected trace elements in deciduous forest throughfall, Atmos. Environ., 35(20), 3453–3462,
738 doi:10.1016/S1352-2310(01)00133-9, 2001.

739 Rea, A. W., Lindberg, S. E., Scherbatskoy, T. and Keeler, G. J.: Mercury accumulation in foliage over
740 time in two northern mixed-hardwood forests, Water Air Soil Poll., 133, 49–67, 2002.

741 Reich, P. B., Walters, M. B. and Ellsworth, D. S.: From tropics to tundra: Global convergence in plant
742 functioning, P. Natl. A. Sci. USA, 94(25), 13730–13734, doi:10.1073/pnas.94.25.13730, 1997.

743 Risch, M. R., DeWild, J. F., Krabbenhoft, D. P., Kolka, R. K. and Zhang, L.: Litterfall mercury dry
744 deposition in the eastern USA, Environ. Pollut., 161, 284–290, doi:10.1016/j.envpol.2011.06.005,
745 2012.

746 Risch, M. R., DeWild, J. F., Gay, D. A., Zhang, L., Boyer, E. W. and Krabbenhoft, D. P.:
747 Atmospheric mercury deposition to forests in the eastern USA, Environ. Pollut., 228, 8–18,
748 doi:10.1016/j.envpol.2017.05.004, 2017.

749 Robakowski, P. and Bielinis, E.: Needle age dependence of photosynthesis along a light gradient
750 within an Abies alba crown, Acta Pysiol. Plant., 39(3), doi:10.1007/s11738-017-2376-y, 2017.

751 Rötzer, T. and Chmielewski, F.: Phenological maps of Europe, Clim. Res., 18, 249–257,
752 doi:10.3354/cr018249, 2001.

753 Rutter, A. P., Schauer, J. J., Shafer, M. M., Creswell, J. E., Olson, M. R., Robinson, M., Collins, R.
754 M., Parman, A. M., Katzman, T. L. and Mallek, J. L.: Dry deposition of gaseous elemental mercury to

https://doi.org/10.5194/bg-2020-289
Preprint. Discussion started: 26 August 2020

755 plants and soils using mercury stable isotopes in a controlled environment, Atmos. Environ., 45(4),
756 848–855, doi:10.1016/j.atmosenv.2010.11.025, 2011.

757 Saiz-Lopez, A., Sitkiewicz, S. P., Roca-Sanjuán, D., Oliva-Enrich, J. M., Dávalos, J. Z., Notario, R.,
758 Jiskra, M., Xu, Y., Wang, F., Thackray, C. P., Sunderland, E. M., Jacob, D. J., Travnikov, O., Cuevas,
759 C. A., Acuña, A. U., Rivero, D., Plane, J. M. C., Kinnison, D. E. and Sonke, J. E.: Photoreduction of
760 gaseous oxidized mercury changes global atmospheric mercury speciation, transport and deposition,
761 Nat. Commun., 9(1), 1–9, doi:10.1038/s41467-018-07075-3, 2018.

762 Schleyer, R., Bieber, E. and Wallasch, M.: Das Luftmessnetz des Umweltbundesamtes (In German),
763 UBA German Federal Environment Agency, 2013.

764 Schuldt, B., Buras, A., Arend, M., Vitasse, Y., Beierkuhnlein, C., Damm, A., Gharun, M., Grams, T.
765 E. E., Hauck, M., Hajek, P., Hartmann, H., Hiltbrunner, E., Hoch, G., Holloway-Phillips, M., Körner,
766 C., Larysch, E., Lübbe, T., Nelson, D. B., Rammig, A., Rigling, A., Rose, L., Ruehr, N. K.,
767 Schumann, K., Weiser, F., Werner, C., Wohlgemuth, T., Zang, C. S. and Kahmen, A.: A first
768 assessment of the impact of the extreme 2018 summer drought on Central European forests, Basic
769 Appl. Ecol., 45, 86–103, doi:10.1016/j.baae.2020.04.003, 2020.

770 Schulze, E. D.: Carbon dioxide and water vapor exchange in response to drought in the atmosphere
771 and in the soil, Ann. Rev. Plant Physiol., 37, 28, 1986.

772 Sharma, R. P., Vacek, Z. and Vacek, S.: Individual tree crown width models for Norway spruce and
773 European beech in Czech Republic, Forest Ecol. Manag., 366, 208–220,
774 doi:10.1016/j.foreco.2016.01.040, 2016.

775 Sonnewald, U.: Physiology of Development, in Strasburger's Plant Sciences, pp. 411–530, Springer
776 Berlin Heidelberg, Berlin, Heidelberg., 2013.

777 Sprovieri, F., Pirrone, N., Bencardino, M., D'Amore, F., Angot, H., Barbante, C., Brunke,
778 E.-G., Arcega-Cabrera, F., Cairns, W., Comero, S., Diéguez, M. del C., Dommergue, A., Ebinghaus,
779 R., Feng, X. B., Fu, X., Garcia, P. E., Gawlik, B. M., Hageström, U., Hansson, K., Horvat, M.,
780 Kotnik, J., Labuschagne, C., Magand, O., Martin, L., Mashyanov, N., Mkololo, T., Munthe, J.,
781 Obolkin, V., Ramirez Islas, M., Sena, F., Somerset, V., Spandow, P., Vardè, M., Walters, C.,
782 Wängberg, I., Weigelt, A., Yang, X. and Zhang, H.: Five-year records of mercury wet deposition flux
783 at GMOS sites in the Northern and Southern hemispheres, Atmos. Chem. Phys., 17(4), 2689–2708,
784 doi:10.5194/acp-17-2689-2017, 2017.

785 St. Louis, V. L., Rudd, J. W. M., Kelly, C. A., Hall, B. D., Rolfhus, K. R., Scott, K. J., Lindberg, S. E.
786 and Dong, W.: Importance of the forest canopy to fluxes of methyl mercury and total mercury to
787 boreal ecosystems, Environ. Sci. Technol., 35(15), 3089–3098, doi:10.1021/es001924p, 2001.

788 Stamenkovic, J. and Gustin, M. S.: Nonstomatal versus Stomatal Uptake of Atmospheric Mercury,
789 Environ. Sci. Technol., 43(5), 1367–1372, doi:10.1021/es801583a, 2009.

790 Stancioiu, P. T. and O'Hara, K. L.: Morphological plasticity of regeneration subject to different levels
791 of canopy cover in mixed-species, multiaged forests of the Romanian Carpathians, Trees, 20(2), 196–
792 209, doi:10.1007/s00468-005-0026-2, 2006.

793 Tahvanainen, T. and Forss, E.: Individual tree models for the crown biomass distribution of Scots
794 pine, Norway spruce and birch in Finland, Forest Ecol. Manag., 255(3), 455–467,
795 doi:10.1016/j.foreco.2007.09.035, 2008.

796 Teixeira, D. C., Montezuma, R. C., Oliveira, R. R. and Silva-Filho, E. V.: Litterfall mercury
797 deposition in Atlantic forest ecosystem from SE – Brazil, Environ. Pollut., 164, 11–15,
798 doi:10.1016/j.envpol.2011.10.032, 2012.

https://doi.org/10.5194/bg-2020-289
Preprint. Discussion started: 26 August 2020

799 Temesgen, H., LeMay, V. and Mitchell, S. J.: Tree crown ratio models for multi-species and multi-
800 layered stands of southeastern British Columbia, Forest Chron., 81(1), 133–141,
801 doi:10.5558/tfc81133-1, 2005.

802 Tyrrell, M. L., Ross, J. and Kelty, M.: Carbon dynamics in the Temperate Forest, in Managing Forest
803 Carbon in a Changing Climate, edited by M. S. Ashton, M. L. Tyrrell, D. Spalding, and B. Gentry, pp.
804 77–107, Springer Netherlands, Dordrecht., 2012.

805 UN Environment: Global Mercury Assessment Report 2018. UN Environmental Programme,
806 Chemicals and Health Branch Geneva, Switzerland, [online] Available from:
807 https://wedocs.unep.org/bitstream/handle/20.500.11822/27579/GMA2018.pdf?sequence=1&isAllowe
808 d=y (Accessed 2 October 2019), 2019.

809 Wang, X., Bao, Z., Lin, C.-J., Yuan, W. and Feng, X.: Assessment of global mercury deposition
810 through litterfall, Environ. Sci. Technol., 50(16), 8548–8557, doi:10.1021/acs.est.5b06351, 2016.

811 Wängberg, I. and Munthe, J.: Atmospheric mercury in Sweden, Northern Finland and Northern
812 Europe. Results from national monitoring and European research., IVL Swedish Environmental
813 Research Institute report, 2001.

814 Wängberg, I., Munthe, J., Berg, T., Ebinghaus, R., Kock, H. H., Temme, C., Bieber, E., Spain, T. G.
815 and Stolk, A.: Trends in air concentration and deposition of mercury in the coastal environment of the
816 North Sea Area, Atmos. Environ., 41(12), 2612–2619, doi:10.1016/j.atmosenv.2006.11.024, 2007.

817 Wängberg, I., Nerentorp Mastromonaco, M. G., Munthe, J. and Gårdfeldt, K.: Airborne mercury
818 species at the Råö background monitoring site in Sweden: distribution of mercury as an effect of long-
819 range transport, Atmos. Chem. Phys., 16(21), 13379–13387, doi:10.5194/acp-16-13379-2016, 2016.

820 Warren, C. R.: Why does photosynthesis decrease with needle age in Pinus pinaster?, Trees, 20(2),
821 157–164, doi:10.1007/s00468-005-0021-7, 2006.

822 Weiss-Penzias, P. S., Gay, D. A., Brigham, M. E., Parsons, M. T., Gustin, M. S. and ter Schure, A.:
823 Trends in mercury wet deposition and mercury air concentrations across the U.S. and Canada, Sci.
824 Total Environ., 568, 546–556, doi:10.1016/j.scitotenv.2016.01.061, 2016.

825 Wieser, G. and Tausz, M., Eds.: Trees at their Upper Limit: Treelife Limitation at the Alpine
826 Timberline, Springer Netherlands, Dordrecht., 2007.

827 Wright, I. J., Reich, P. B., Westoby, M., Ackerly, D. D., Baruch, Z., Bongers, F., Cavender-Bares, J.,
828 Chapin, T., Cornelissen, J. H. C., Diemer, M., Flexas, J., Garnier, E., Groom, P. K., Gulias, J.,
829 Hikosaka, K., Lamont, B. B., Lee, T., Lee, W., Lusk, C., Midgley, J. J., Navas, M.-L., Niinemets, Ü.,
830 Oleksyn, J., Osada, N., Poorter, H., Poot, P., Prior, L., Pyankov, V. I., Roumet, C., Thomas, S. C.,
831 Tjoelker, M. G., Veneklaas, E. J. and Villar, R.: The worldwide leaf economics spectrum, Nature,
832 428(6985), 821–827, doi:10.1038/nature02403, 2004.

833 Wright, L. P., Zhang, L. and Marsik, F. J.: Overview of mercury dry deposition, litterfall, and
834 throughfall studies, Atmospheric Chemistry and Physics, 16(21), 13399–13416, 2016.

835 Xiao, C.-W., Janssens, I. A., Curiel Yuste, J. and Ceulemans, R.: Variation of specific leaf area and
836 upscaling to leaf area index in mature Scots pine, Trees, 20(3), 304, doi:10.1007/s00468-005-0039-x,
837 2006.

838 Yang, Y., Yanai, R. D., Montesdeoca, M. and Driscoll, C. T.: Measuring mercury in wood:
839 challenging but important, Int. J. Environ. An. Ch., 97(5), 456–467,
840 doi:10.1080/03067319.2017.1324852, 2017.

https://doi.org/10.5194/bg-2020-289
Preprint. Discussion started: 26 August 2020

841 Yuan, W., Sommar, J., Lin, C.-J., Wang, X., Li, K., Liu, Y., Zhang, H., Lu, Z., Wu, C. and Feng, X.:
842 Stable isotope evidence shows re-emission of elemental mercury vapor occurring after reductive loss
843 from foliage, Environ. Sci. Technol., 53(2), 651–660, doi:10.1021/acs.est.8b04865, 2019.

844 Zhang, L., Wright, L. P. and Blanchard, P.: A review of current knowledge concerning dry deposition
845 of atmospheric mercury, Atmos. Environ., 43(37), 5853–5864, doi:10.1016/j.atmosenv.2009.08.019,
846 2009.

847 Zhang, L., Wu, Z., Cheng, I., Wright, L. P., Olson, M. L., Gay, D. A., Risch, M. R., Brooks, S.,
848 Castro, M. S., Conley, G. D., Edgerton, E. S., Holsen, T. M., Luke, W., Tordon, R. and Weiss-
849 Penzias, P.: The estimated six-year mercury dry deposition across North America, Environ. Sci.
850 Technol., 50(23), 12864–12873, doi:10.1021/acs.est.6b04276, 2016.

851 Zheng, W., Obrist, D., Weis, D. and Bergquist, B. A.: Mercury isotope compositions across North
852 American forests, Global Biochem. Cy., 30(10), 1475–1492, doi:10.1002/2015GB005323, 2016.

853